NeuroImage: Clinical 20 (2018) 286–296

Contents lists available at ScienceDirect

NeuroImage: Clinical

journal homepage: www.elsevier.com/locate/ynicl

Left lateralized cerebral glucose metabolism declines in amyloid-β positive persons with mild cognitive impairment

Christopher M. Weise[a,*], Kewei Chen[b,e,h], Yinghua Chen[b,h], Xiaoying Kuang[b,h], Cary R. Savage[b,f], Eric M. Reiman[b,c,d,e,g,h], for the Alzheimer's Disease Neuroimaging Initiative[1]

[a] Department of Neurology, University of Leipzig, Germany
[b] Banner Alzheimer's Institute, Phoenix, AZ, USA
[c] School of Mathematics and Statistics (KC), Neurodegenerative Disease Research Center (EMR), Arizona State University, USA
[d] Department of Neurology, College of Medicine – Phoenix (KC), Department of Psychiatry (EMR), University of Arizona, USA
[e] Neurogenomics Division, Translational Genomics Research Institute, University of Arizona, Arizona State University, Phoenix, AZ, USA
[f] Center for Brain, Biology and Behavior, Department of Psychology, University of Nebraska, Lincoln, NE, USA
[g] Banner-Arizona State University, Neurodegenerative Disease Research Center, BioDesign Institute, Arizona State University, Tempe, AZ, USA
[h] Arizona Alzheimer's Consortium, Phoenix, AZ, USA

ARTICLE INFO

Keywords:
Alzheimer's disease
FDG PET
MCI
Lateralization

ABSTRACT

Background: Previous publications indicate that Alzheimer's Disease (AD) related cortical atrophy may develop in asymmetric patterns, with accentuation of the left hemisphere. Since fluorodeoxyglucose positron emission tomography (FDG PET) measurements of the regional cerebral metabolic rate of glucose (rCMRgl) provide a sensitive and specific marker of neurodegenerative disease progression, we sought to investigate the longitudinal pattern of rCMRgl in amyloid-positive persons with mild cognitive impairment (MCI) and dementia, hypothesizing asymmetric declines of cerebral glucose metabolism.

Methods: Using florbetapir PET and cerebrospinal fluid (CSF) measures to define amyloid-β (Aβ) positivity, 40 Aβ negative (Aβ-) cognitively unimpaired controls (CU; 76 ± 5y), 76 Aβ positive (Aβ+) persons with MCI (76 ± 7y) and 51 Aβ + persons with probable AD dementia (75 ± 7y) from the AD Neuroimaging Initiative (ADNI) were included in this study with baseline and 2-year follow-up FDG PET scans. The degree of lateralization of longitudinal rCMRgl declines in subjects with Aβ + MCI and AD in comparison with Aβ- CU were statistically quantified via bootstrapped lateralization indices [(LI); range − 1 (right) to 1 (left)].

Results: Compared to Aβ- CU, Aβ + MCI patients showed marked left hemispheric lateralization (LI: 0.78). In contrast, modest right hemispheric lateralization (LI: −0.33) of rCMRgl declines was found in Aβ + persons with probable AD dementia. Additional comparisons of Aβ + groups (i.e. MCI and probable AD dementia) consequently indicated right hemispheric lateralization (LI: −0.79) of stronger rCMRgl declines in dementia stages of AD. For all comparisons, voxel-based analyses confirmed significant (pFWE < 0.05) declines of rCMRgl within AD-typical brain regions. Analyses of cognitive data yielded predominant decline of memory functions in both MCI and dementia stages of AD.

Conclusions: These data indicate that in early stages, AD may be characterized by a more lateralized pattern of left hemispheric rCMRgl declines. However, metabolic differences between hemispheres appear to diminish with further progression of the disease.

1. Introduction

Alzheimer's disease (AD) is the most common cause of cognitive impairment in older persons. In recent years, AD has been conceptualized as a progressive sequence of pathophysiological changes that include the extracellular accumulation of amyloid-β (Aβ), tau-mediated neuronal dysfunction/death and brain atrophy that correspond roughly to cognitively unimpaired, mild cognitive impairment

* Corresponding author at: University of Leipzig, Department of Neurology, Liebigstr. 20, 04103 Leipzig, Germany.
E-mail address: christopher.weise@medizin.uni-leipzig.de (C.M. Weise).

[1] Data used in preparation of this article were obtained from the Alzheimer's Disease Neuroimaging Initiative (ADNI) database (adni.loni.usc.edu). As such, the investigators within the ADNI contributed to the design and implementation of ADNI and/or provided data but did not participate in analysis or writing of this report. A complete listing of ADNI investigators can be found at http://adni.loni.usc.edu/wp-content/uploads/how_to_apply/ADNI_Acknowledgement_List.pdf.

https://doi.org/10.1016/j.nicl.2018.07.016
Received 5 June 2018; Received in revised form 10 July 2018; Accepted 16 July 2018
Available online 17 July 2018

(MCI) and dementia stages (Jack et al. 2011, 2018).

Brain imaging measurements have been used to detect and track Aβ, tau, and neurodegenerative features of AD in the preclinical (cognitively unimpaired), MCI and dementia stages. The best established examples include PET measurements of fibrillar Aβ deposition, PET measurements of paired helical filament (PHF) tau deposition, MRI measurements of hippocampal and whole brain atrophy, and fluorodeoxyglucose PET measurements of regional cerebral metabolic rate for glucose (rCMRgl) decline in brain regions preferentially affected by AD (Herholz and Ebmeier 2011; Reiman and Jagust 2012; Saint-Aubert et al. 2017). In the most recent conceptualization (Jack et al. 2018), biomarker evidence of amyloid-β (Aβ) pathology reflects "AD pathophysiological change", biomarker evidence of both amyloid-β and tau pathology reflects "AD", and individuals can also be characterized in terms of the evidence of neurodegenerative disease changes that may include rCMRgl declines and brain atrophy (i.e., "AT(N)" research criteria for AD; Jack et al. 2018)).

AD and related disorders are associated with distinctive MRI and FDG PET patterns of neurodegeneration. Some neurodegenerative diseases appear to begin with or are characterized by asymmetric patterns of neurodegeneration (e.g., Parkinson's Disease (PD) and Primary Progressive Aphasia (PPA), (Claassen et al. 2016; Gorno-Tempini et al. 2004). While AD has been characterized by bilateral neurodegenerative disease changes in medial temporal and heteromodal sensory association areas, several neuroimaging studies have suggested a pronunciation of the left hemisphere with respect to amyloid deposition (Raji et al. 2008) gray matter atrophy (Janke et al. 2001; Shi et al. 2009; Thompson et al. 1998, 2001), cerebral perfusion and metabolism (Friedland et al. 1985; Loewenstein et al. 1989; Volkow et al. 2002) in persons with AD. Whereas many of these findings (particularly from studies of brain metabolism) have been cross-sectional, we sought to investigate the possibility that amyloid-β positive (Aβ+) persons might demonstrate asymmetric left lateralized longitudinal patterns of neurodegeneration, especially during the earlier clinical stages of AD. To address this possibility we compared longitudinal patterns of rCMRgl declines in Aβ + probable AD dementia, MCI and an amyloid-β negative (Aβ-) cognitively unimpaired control group from the AD Neuroimaging Initiative (ADNI).

2. Subjects and methods

2.1. Subjects

Participant data for this study were drawn from the ADNI dataset, an ongoing longitudinal study (currently ADNI-3) devoted to the establishment of biological and neuroimaging biomarkers of MCI and Alzheimer's disease. Detailed information on participant recruitment, inclusion- and exclusion criteria are provided on the ADNI website (www.adni-info.org/index.php). In order to maximise the sensitivity of our analyses we only included amyloid-β negative (Aβ-) cognitively unimpaired control subjects (CU) based on CSF measures (threshold > 192) or florbetapir PET (threshold < 1.18) with cerebellum reference region, thereby optimally avoiding the inclusion of subjects with preclinical and asymptomatic stages of AD. Similarly only amyloid-β positive (Aβ+) MCI and AD patients were included, thus avoiding misclassification of patients and maximising the probability of AD pathology being the underlying cause of cognitive impairment. In total, we selected a sample of $n = 167$ subjects, based on availability of longitudinal FDG PET scans and information on amyloid pathology, resulting in a sample of 51 Aβ + subjects with AD dementia, 76 Aβ + subjects with MCI, and 40 Aβ- CU. In the following, we will refer to MCI-AD and dementia-AD for MCI and dementia subjects with evidence of AD pathology.

2.2. Clinical evaluation

For each subject, cognitive function was evaluated at each visit (for details please see www.adni-info.org). Measures of cognitive function included - next to others - the Auditory Verbal Learning Test [AVLT; (Rey 1964)] Total and Long-Term Memory (LTM) scores, CDR sum of boxes (CDR-SOB; (Morris 1993)), MMSE (Folstein et al. 1975), Category Fluency (animals) (Rosen 1980) and the modified AD Assessment Scale-Cognitive Subscale (i.e. ADAS-Cog 11/13; Mohs et al. 1997; Rosen et al. 1984). Delta values were calculated for each test and participant. In addition subdomains and individual subitems of the ADAS-cog 13 were analyzed with the goal to further evaluate baseline impairment and subsequent decline of specific cognitive domains. Subitems of the ADAS-cog 13 comprise the following cognitive subdomains: Memory and new learning (i.e. Word Recall, Orientation, Word Recognition, Delayed Word Recall, Recall Instructions), language (i.e. Commands, Naming, Spoken Language, Word Finding, Comprehension), praxis (i.e. Construction, Ideational Praxis) and processing speed (i.e. Number Cancellation) with higher scores indicating worse performance. For the item "Number Cancellation" data points were missing for $N = 5$ subjects ($N = 4$ dementia-AD; $N = 1$ CU). Since individual subitems of the ADAS-cog 13 differ with respect to the maximum possible value, results were illustrated as percentage of the maximum possible scores. Non-imaging data were analyzed using ANOVA or Chi Square whenever applicable. For post-hoc between group comparisons Duncan's multiple range test was applied. Results are reported at alpha 0.05 uncorrected.

2.3. Imaging procedures

Longitudinal imaging data from different participating sites were subjected to a standardized protocol (http://www.loni.ucla.edu/ADNI/Data/ADNI_Data.shtml) of measured-attenuation correction and specific reconstruction algorithms in order to account for site specific differences. These preprocessing steps were performed by the ADNI PET Coordinating Center at the University of Michigan made available for download at the LONI ADNI website. After download of PET images additional pre-processing steps were performed using SPM5 (http://www.fil.ion.ucl.ac.uk/spm), including deformation into a standard space of the Talairach atlas and spatial smoothing with a 3-dimensional Gaussian filter with 8 mm full width at half maximum. Next, subtraction images of the FDG scans scaled by the global counts were calculated (i.e. baseline/global_at_baseline – followup/global_at_followup) for characterization and comparisons of 24-month rCMRgl declines.

To test the hypothesis of lateralized longitudinal declines of rCMRgl declines we used SPM8 (www.fil.ion.ucl.ac.uk) and the LI-toolbox (Wilke and Lidzba 2007). First, SPM8 was used for voxel-based analyses of rCMRgl declines by applying either two-sample *t*-test for group comparisons or one sample *t*-tests for within group analyses to the above mentioned subtraction images. In addition, post-hoc regression analyses were performed to investigate associations of cognitive decline [(i.e. ADAS-cog 13 and Category Fluency (animals)] with rCMRgl declines in dementia-AD and MCI-AD subjects. Then, SPM derived T-maps were analyzed with the LI-toolbox by calculating an overall weighted bootstrapped lateralization index (LI) for the unthresholded maps. This approach combines the commonly used lateralization eq. (LI = (left-right)/(left + right)) with adaptive thresholding and automated bootstrapping algorithms to minimize the impact of outliers. For our analyses we furthermore used an inclusive standard gray matter mask and an additional exclusive mask (i.e. midline +/− 5 mm) as provided by the LI-toolbox, in order to reduce noise related artifacts. For the calculated LI weighted means (LIwm), negative values indicate right hemispheric lateralization and positive values indicate left hemispheric lateralization. Based on the LIwm, lateralization was classified as either absent (LIwm −0.25 to 0.25), weak (LIwm −0.25 to −0.50 and 0.25 to 0.50) or strong (LIwm < −0.50 and > 0.50) (e.g. De Winter et al. 2015). Importantly, this approach largely avoids the introduction of

arbitrary thresholds and strongly reduces the impact of potential outliers.

The main goal of this study was to statistically quantify lateralization of longitudinal rCMRgl declines, by using a global index that provides information free of the type-1 error due to multiple comparisons, via the above mentioned analytical approach (i.e. the bootstrapped lateralization indices for unthresholded maps). Since the introduction of conservative thresholds may artificially create the impression of lateralization, maps of rCMRgl declines were displayed with an uncorrected voxelwise threshold of $p < .005$. Nevertheless, additional information on whole-brain corrected results (FWE correction on the cluster-level; FWE_c) is provided in the respective tables.

Detailed results of within group analyses and regression are additionally provided as supplementary information. Results of the within group one-sample *t*-tests of rCMRgl declines in MCI-AD and dementia-AD patients are reported at $p < .05$ FWE voxel-level corrected (FWE_v), to avoid excessive clustering and provide better information on the anatomical pattern of rCMRgl declines.

3. Results

3.1. Subject characteristics and cognitive performance

The subject groups' baseline characteristics are summarized in Table 1, data of 24-month cognitive changes are provided as supplementary data (Table S1). No significant differences were observed for baseline age, gender distribution, education and time interval between groups. As expected, in comparison with the CU group, the dementia-AD and MCI-AD groups had a higher proportion of APOE4 carriers, lower baseline cognitive performance, and greater 24-month cognitive declines. For the sub-items of the ADAS-cog 13 at baseline (illustrated in Fig. 1), most prominent deficits were observed for memory functions [i.e. Delayed Word Recall, Word Recall, Word Recognition (all dementia-AD > MCI-AD > CU) and Orientation (dementia-AD > MCI-AD/CU)], Processing Speed [i.e. Number Cancellation (dementia-AD > MCI-AD > CU)] and Praxis [i.e. Construction (dementia-AD > MCI-AD > CU)], while only minor deficits were evident for language functions [i.e. Word Finding and Naming (all dementia-AD/MCI-AD > CU]. Similar results were seen when the respective subitems were grouped as subdomains, again with most prominent deficits in the memory subdomain (dementia-AD > MCI-AD > CU) and less profound deficits in the praxis and language subdomain (dementia-AD > MCI-AD > CU and dementia-AD/MCI-AD > CU). During the 2 year follow up period cognitive decline again was most evident for memory functions [i.e. Orientation (dementia-AD > MCI-AD > CU)], Word Recall, Delayed Word Recall, Word Recognition (all 3 items dementia-AD/MCI-AD > CU) and Recall Instructions (dementia-AD > MCI-AD/CU), followed by Praxis (i.e. Ideational Praxis (dementia-AD > MCI-AD/CU) and language functions [i.e. Word Finding, Naming, Commands, Comprehension (all dementia-AD > MCI-AD/CU) and Spoken Language (dementia-AD > CU)]. Analyses of the ADAS subdomains yielded significant decline within the memory subdomain for both AD and MCI subjects (dementia-AD > MCI-AD > CU) and within the language and praxis subdomain for AD subjects only (both dementia-AD > MCI-AD/CU).

For Category Fluency (animals) significant deficits were found at baseline for dementia-AD and MCI-AD (dementia-AD > MCI-AD > CU) with weakly significant 24-month decline (dementia-AD/MCI-AD > CU).

3.2. 24-month rCMRgl declines

Compared to CU, MCI-AD patients showed rCMRgl declines predominantly located within the left lateral temporal cortex

Table 1
Baseline subject characteristics.

	CU Aβ-	MCI Aβ+	AD Aβ+	*P* value
	(*n* = 40)	(*n* = 76)	(*n* = 51)	
Baseline age	76.1 ± 5.3	75.8 ± 6.8	75.2 ± 7.1	n.s.
*Gender (M/F)	20/20	51/25	31/20	n.s.
Education (years)	15.5 ± 3.2	16.3 ± 2.859	15.3 ± 3.2	n.s.
Timeinterval (years)	1.99 ± 0.26	1.95 ± 0.26	1.84 ± 0.44	n.s
*APOE E4 gene dose (NC/HT/HM)	32/8/0	32/30/14	8/28/15	4.98E-08
MMSE	28.6 ± 1.5	26.9 ± 1.9	23.4 ± 1.9	2.09E-29
CDR-SOB	0.1 ± 0.2	1.7 ± 1.0	4.3 ± 1.5	7.80E-43
AVLT-STM	8.3 ± 3.3	3.6 ± 3.1	1.4 ± 1.6 (50)	2.76E-22
AVLT-LTM	7.5 ± 3.8	2.1 ± 3.0	0.6 ± 1.5	4.62E-23
AVLT-Total	42.2 ± 9.2	29.4 ± 8.1	22.8 ± 6.8 (50)	1.05E-21
Category fluency (animals)	19.8 ± 4.8	15.5 ± 3.9	13.3 ± 4.2	1.03E-10
ADAS-cog 13	10.1 ± 4.5 (39)	20.0 ± 5.9	28.7 ± 7.6 (50)	6.89E-29
ADAS-cog 11	6.4 ± 3.0	12.1 ± 4.2	18.0 ± 6.0	6.94E-23
ADAS memory subdomain (0–45)	8.8 ± 4.3	17.0 ± 5.8	23.8 ± 5.9	7.47E-26
ADAS language subdomain (0–25)	0.3 ± 0.6	1.2 ± 1.2	1.4 ± 1.8	2.05E-04
ADAS praxis subdomain (0 − 10)	0.4 ± 0.6	0.7 ± 0.7	1.3 ± 0.8	1.29E-08
ADAS Q1 word recall (0–10)	3.0 ± 1.2	4.8 ± 1.2	6.0 ± 1.4	1.95E-21
ADAS Q2 commands (0–5)	0.1 ± 0.3	0.2 ± 0.5	0.3 ± 0.5	n.s.
ADAS Q3 construction (0–5)	0.3 ± 0.5	0.6 ± 0.6	1.0 ± 0.7	1.86E-07
ADAS Q4 delayed word recall (0–10)	3.1 ± 1.9	6.7 ± 2.3	8.5 ± 1.7	3.91E-25
ADAS Q5 naming (0–5)	0.1 ± 0.3	0.3 ± 0.5	0.3 ± 0.5	0.008
ADAS Q6 Ideational Praxis (0–5)	0.1 ± 0.3	0.1 ± 0.3	0.2 ± 0.4	< 0.05
ADAS Q7 orientation (0–8)	0.2 ± 0.4	0.5 ± 0.8	2.5 ± 1.7	7.42E-21
ADAS Q8 word recognition (0 − 12)	2.6 ± 2.4	4.9 ± 3.0	6.7 ± 3.0	8.41E-10
ADAS Q9 recall instructions (0–5)	0.0 ± 0.2	0.1 ± 0.4	0.1 ± 0.4	n.s.
ADAS Q10 spoken language (0–5)	0.1 ± 0.2	0.1 ± 0.4	0.2 ± 0.6	n.s.
ADAS Q11 word finding (0–5)	0.1 ± 0.2	0.4 ± 0.6	0.5 ± 0.8	0.004
ADAS Q12 comprehension (0–5)	0.0 ± 0.2	0.1 ± 0.3	0.1 ± 0.5	n.s.
ADAS Q14 number cancellation (0–5)	0.5 ± 0.7(39)	1.1 ± 0.7	2.2 ± 1.5 (50)	1.14E-13

Data is presented as mean ± SD except for *.Group differences were assessed by ANOVA except for * (i.e. Chi-squared test); *NC* noncarriers; *HT* heterozygotes; *HM* homozygotes; *ADAS-cog* Alzheimer's Disease Assessment Scale-cognitive subscale; *MMSE* Mini-Mental State Examination; *CDR-SOB* Clinical Dementia Rating Scale Sum of Boxes; *AVLT* Auditory Verbal Learning Test; *STM* short term memory; *LTM* long term memory.

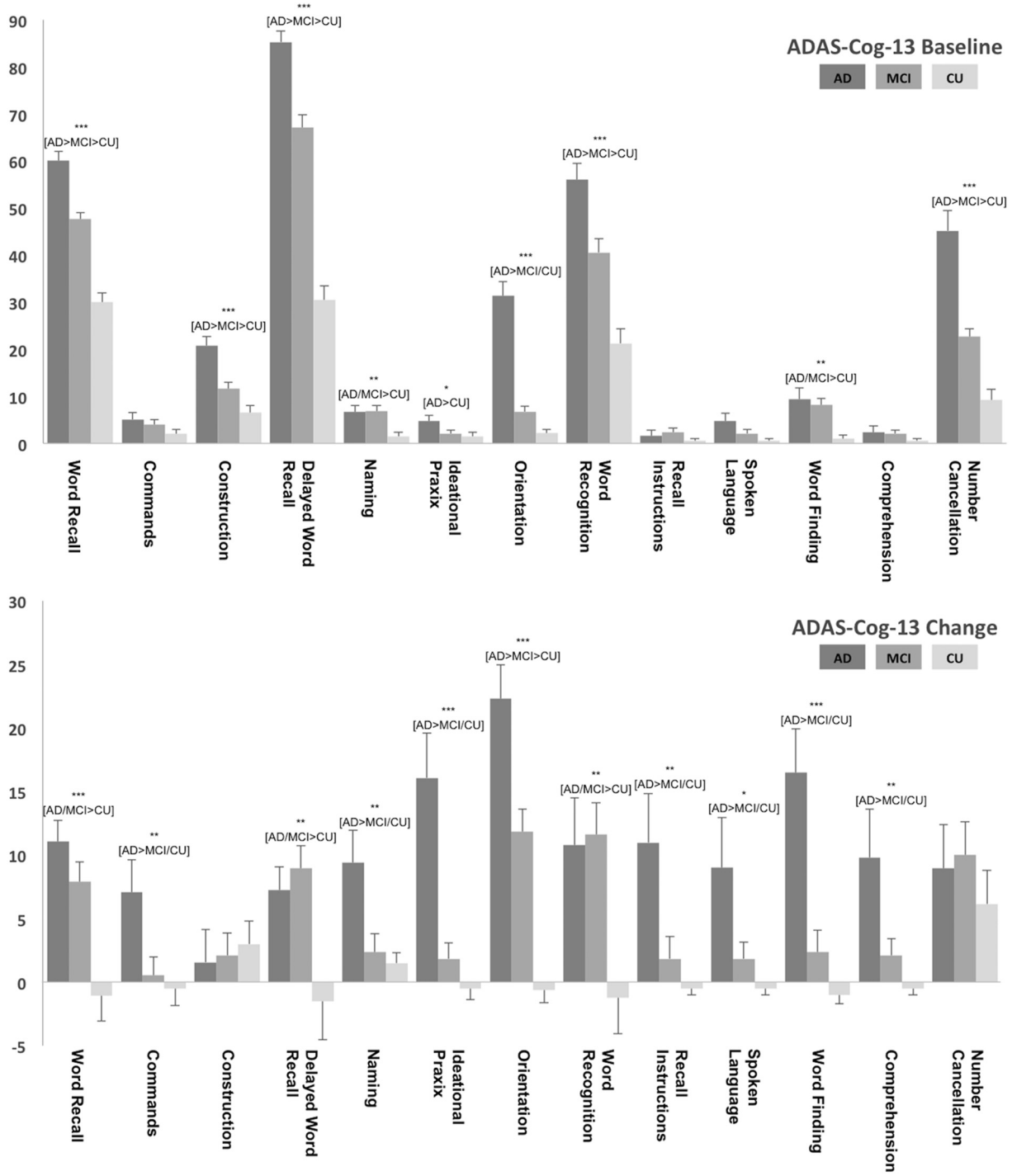

Fig. 1. Mean baseline performance (top chart) and change over 24 months (bottom chart) for the ADAS-cog 13 subitems for dementia-AD (AD), MCI-AD (MCI) and cognitively unimpaired (CU) subjects. Results are illustrated as percentage of the maximum possible value, with higher values indicating worse performance. Significant group differences are indicated by * (ANOVA: $*p < .5$; $**p < .001$; $***p < .0001$; for detailed *p*-values see Table 1 and Table S1) with the corresponding between group differences below in brackets (i.e. Duncan's multiple range test).

($pFWE_c < 0.05$) (see Fig. 2 and Table 2). This pattern of rCMRgl decline was found to be strongly left lateralized (LIwm 0.78).

Subjects with dementia-AD in comparison to CU exhibited bilateral declines of rCMRgl (see Fig. 3 and Table 3), predominantly within the temporal cortices (lateral > medial), the parietal lobes (i.e. bilateral inferior parietal lobule), precuneus and the posterior cingulate (all $pFWE_c < 0.05$) with signs of weak right hemispheric lateralization (LIwm −0.33).

Additional comparisons of dementia-AD patients with MCI-AD patients yielded stronger and predominant right hemispheric rCMRgl declines in dementia-AD patients (see Fig. 4 and Table 4), mostly within the right temporal cortex (lateral > medial), the parietal lobe, precuneus, the posterior cingulate (one cluster, $pFWE_c < 0.05$) and the right frontal lobe ($pFWE_c < 0.05$). This pattern of rCMRgl decline was found to be strongly right lateralized (LIwm −0.79).

Within-group analyses yielded rCMRgl declines ($pFWE_v < 0.05$) in MCI-AD and dementia-AD, most prominently within the (posterior) cingulate, the bilateral temporal and parietal lobes and the precuneus

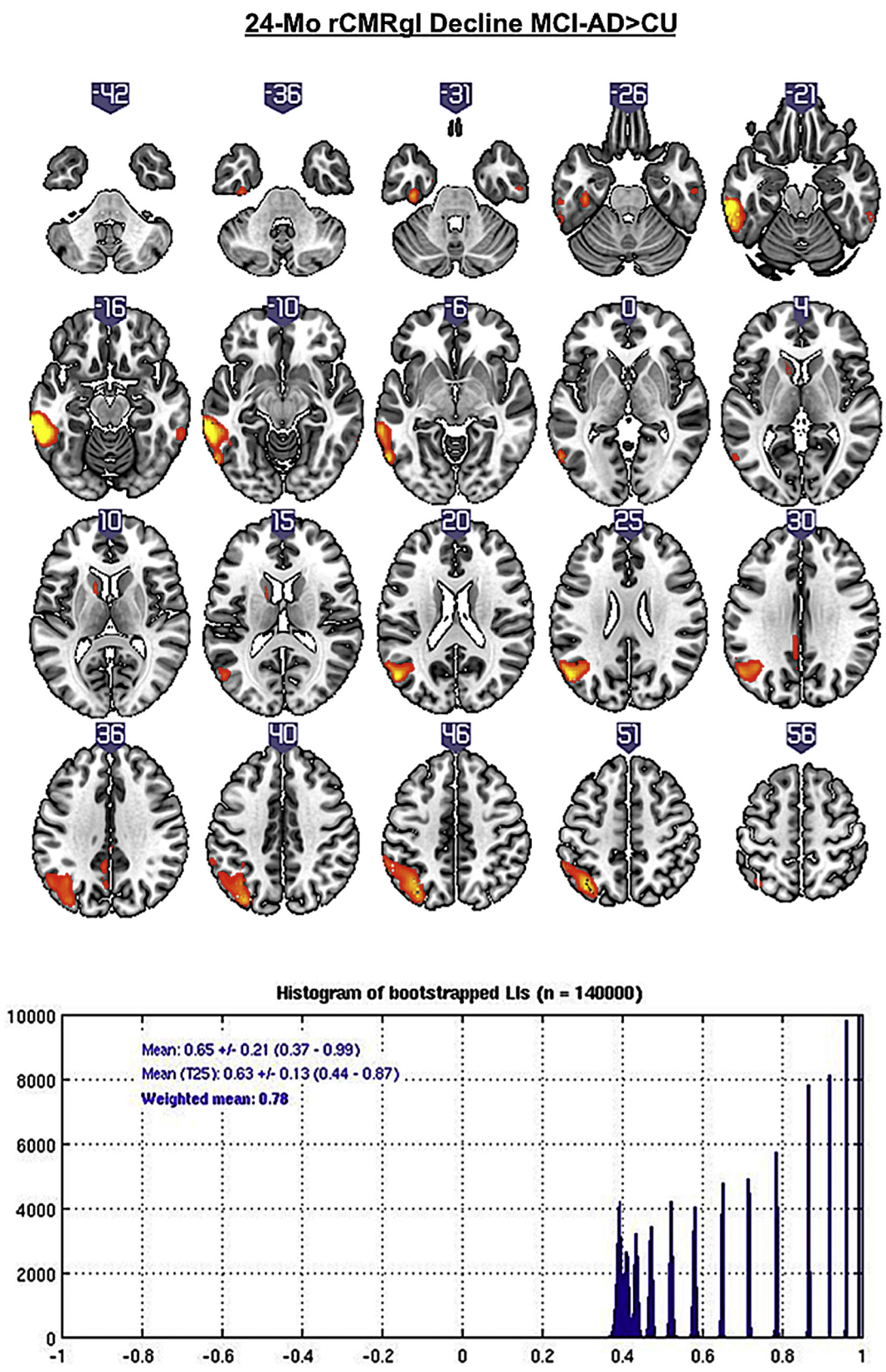

Fig. 2. T-score maps ($p < .005$ uncorrected) of greater 24-month rCMRgl declines in amyloid-β positive MCI-AD patients compared to amyloid-β negative cognitively unimpaired controls (CU) with the corresponding histogram of bootstrapped lateralization indices (LIs).

with signs of weak left hemispheric lateralization for MCI-AD and weak right hemispheric lateralization for dementia-AD (MCI-AD: LIwm 0.46; dementia-AD: LIwm −0.44). rCMRgl declines were also observed in CU subjects, yet less extended and in differing regions (i.e. mostly within frontal and insular cortex and subcortical stuctures; all $pFWE_c < 0.05$) with signs of weak right hemispheric lateralization (CU: LIwm −0.48).

Table 2
24-month rCMRgl declines in amyloid-β positive MCI-AD patients compared to amyloid-β negative cognitively unimpaired controls.

Region		k	p(unc)	MNI (mm)		
				x	y	z
L	**Inferior Temporal Gyrus**	**1362**	**7.95E-06**†	**−64**	**−32**	**−18**
L	Middle Temporal Gyrus		2.11E-05	−60	−46	−14
L	Inferior Temporal Gyrus		0.0002	−58	−64	−8
L	**Middle Temporal Gyrus**	**2200**	**6.47E-05***	**−52**	**−68**	**22**
L	Superior Parietal Lobule		0.0001	−38	−64	50
L	Precuneus		0.0003	−34	−78	42
L	**Parahippocampal Gyrus**	**161**	**0.0004**	**−38**	**−22**	**−30**
L	**Precuneus**	**159**	**0.0014**	**−6**	**−50**	**34**
L	Precuneus		0.0025	−4	−64	34
L	Cingulate Gyrus		0.0040	0	−32	34

Results are listed at $p < .005$ uncorrected and a cluster size threshold of 100 continuous voxels. Bold data indicate primary peaks within a cluster, non-bold data indicate secondary peaks within the cluster. MNI: Montreal Neurological Institute; p(unc): uncorrected p-value; k: cluster size.
* $p < .05$ FWE corrected on the cluster-level.
† $p < .1$ FWE corrected on the cluster-level.

Additional information on within-group analyses is provided as supplementary material (i.e. Table S1–3; Fig. S1–3).

3.3. Associations of 24-month rCMRgl declines with cognitive decline

Post-hoc regression analyses showed that cognitive worsening as measured by the ADAS-cog 13 was associated ($pFWE_c < 0.05$) with rCMRgl declines within the left lateral temporal cortex in MCI-AD. This pattern was found to be strongly left lateralized (LIwm 0.89). In dementia-AD subjects, cognitive worsening was associated with bilateral rCMRgl declines predominantly within the bilateral parietal lobule, precuneus and the posterior cingulate (one large cluster at $pFWE_c < 0.05$) with signs of weak right hemispheric lateralization (LIwm −0.28). Due to missing values in the dementia-AD group ($N = 4$) of Q14 (i.e. number cancellation) of the ADAS-cog 13 additional regression analyses were done with complete data of the ADAS-cog 11 where the same pattern of associations was found (data not shown), similarly with signs of weak right hemispheric lateralization (LIwm −0.33).

Declines of verbal fluency [i.e. Category Fluency (animals)] did not show any significant associations with rCMRgl declines in MCI-AD subjects (all $p > .6$ FWE_c). Uncorrected associations ($p < .005$) were mainly located within the left basal ganglia next to a smaller cluster within the left temporal cortex, overall with signs of strong left lateralization (LIwm = 0.7).

In dementia-AD subjects however, declines of verbal fluency showed significant associations ($p < .05$ FWE_c) with rCMRgl declines within the left precuneus and parietal lobule, the left temporal and frontal cortex. This pattern was found to be strongly left lateralized (LIwm = 0.7). Additional information on regression analyses is provided as supplementary material (i.e. Table S5–6; Fig. S4–6).

4. Discussion

To our knowledge, this is the first longitudinal FDG PET study to investigate asymmetric patterns of rCMRgl decline in MCI and early dementia stages of AD. In a well characterized sample of patients we observed diverging patterns of asymmetric and/or lateralized rCMRgl declines in Aβ + MCI-AD and dementia-AD patients compared to Aβ- cognitively unimpaired controls (CU). While – in comparison to CU - MCI-AD subjects yielded signs of strong left hemispheric lateralization, early stages of dementia-AD were associated with right hemispheric lateralization of rCMRgl, even though this effect was found to be weaker as compared to MCI-AD patients. Consequently, rCMRgl declines in dementia-AD patients compared to MCI-AD patients were found to be strongly right lateralized. Similar directionalities of lateralization were found for within-group analyses of rCMRgl declines in MCI-AD and dementia-AD, however in MCI-AD patients left hemispheric lateralization was weaker as when compared to CU, which in turn showed rCMRgl declines of predominantly prefrontal brain regions with signs of weak right hemispheric lateralization. Importantly, the pattern of rCMRgl declines we observed in MCI-AD and dementia-AD subjects was restricted to brain regions typically affected in AD, thus closely resembling previous FDG-PET studies (e.g. Reiman and Jagust 2012). Although the estimation of lateralization with the LI-Toolbox implies the use of a priori unthresholded imaging data, rCMRgl declines within AD typical regions did reach statistical significance after correction for multiple comparisons, thus providing additional statistical validation.

Additional analyses of cognitive data furthermore showed predominant decline of memory functions for ADAS-cog subitems and subdomains. Importantly, no significant decline of the language subdomain was found for MCI-AD subjects. Post-hoc regression analyses of the 24-month ADAS-cog changes furthermore yielded strong left hemispheric lateralization of its associations with rCMRgl decline. On the other hand, significant decline was found for tests of verbal fluency [i.e. Category fluency (animals)] and results of regression analyses were strongly left lateralized in both dementia-AD and MCI-AD.

FDG PET measurements of rCMRgl have been used in the detection, tracking and differential diagnosis of AD and can be observed long before clinical onset of AD (Reiman and Jagust 2012). Presumed pathophysiological underpinnings of rCMRgl reductions in AD include neuronal and glial derangements of mitochondrial and metabolic functions and consecutive reductions in synaptic function and density (Mosconi 2013). In contrast, earlier upstream pathophysiological events such as amyloid deposition may have plateaued even before clinical signs of AD are noticeable (Jack et al. 2010). Consequently, FDG PET may be more reflective of the clinical course of AD. Importantly, reductions in rCMRgl are sought to precede brain atrophy and alterations in glucose metabolism cannot be solely explained by brain atrophy and increases in CSF spaces (Ibáñez et al. 1998; Jack et al. 2010).

Within the past decades the question whether AD pathology develops in an asymmetric or lateralized fashion has been investigated by numerous studies, yet with conflicting results. While post-mortem studies yielded a high variability of AD pathology for the left and right hemisphere, no clear signs of asymmetry or lateralization were observed (Janota and Mountjoy 1988; Wilcock and Esiri 1987). In contrast, PET measurements of amyloid deposition in MCI and AD patients were found to be weakly left lateralized for some brain regions in MCI and right lateralized in AD, somewhat similar to the pattern of rCMRgl declines we observed in our within-group analyses (Raji et al. 2008). It has to be noted though that these observations were made in a small sample and still require additional confirmation by further studies.

Earlier studies of brain metabolism in AD and subjects at high risk for AD showed asymmetric reductions in cerebral glucose uptake, in parts with predominant left hemispheric metabolic deficits (Friedland et al. 1985; Loewenstein et al. 1989; Siegel et al. 1996; Small et al. 1995) while asymmetric glucose metabolism was found to correlate with cognitive dysfunction of lateralized domains such as language (i.e. left hemisphere) or visuospatial processing (i.e. right hemisphere) (Haxby et al. 1985). Similar observations had been made by Keilp et al. with differing correlations of left and right hemispheric perfusion deficits with specific cognitive domains in AD (Keilp et al. 1996). In addition, more recent studies found marked left hemispheric decrements in FDG uptake in AD patients (Volkow et al. 2002). Consideration of hemispheric differences in AD has also been given in brain structural studies. Observations of accentuated left ventricular enlargement in early AD were – in parts – confirmed by more sophisticated analyses of

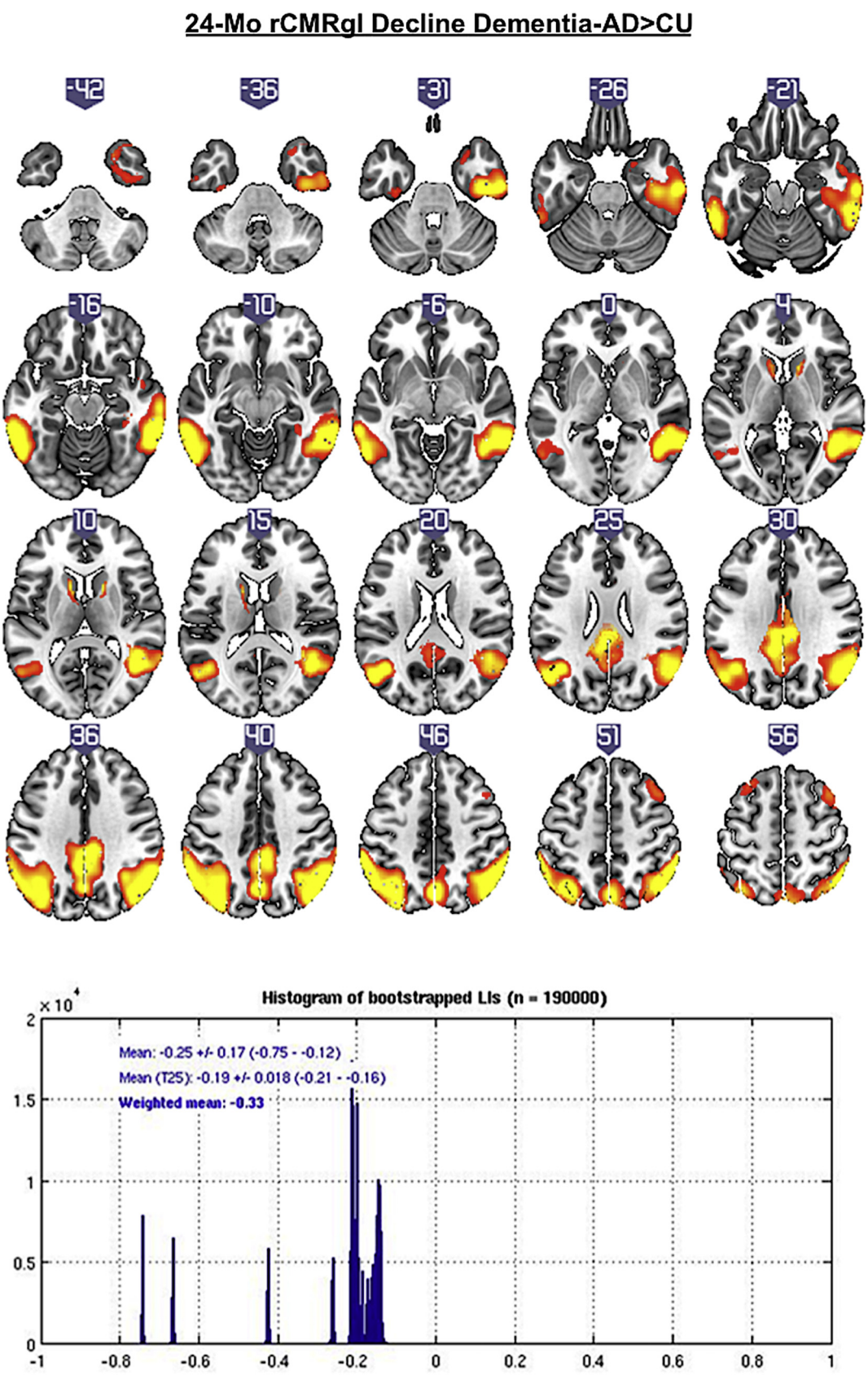

Fig. 3. T-score maps ($p < .005$ uncorrected) of greater 24-month rCMRgl declines in amyloid-β positive dementia-AD patients compared to amyloid-β negative cognitively unimpaired controls (CU) with the corresponding histogram of bootstrapped lateralization indices (LIs).

Table 3
24-month rCMRgl declines in amyloid-β positive dementia-AD patients compared to amyloid-β negative cognitively unimpaired controls.

Region		k	p(unc)	MNI (mm)		
				x	y	z
R	**Inferior Parietal Lobule**	**11,225**	**3.51E-07***	**58**	**−50**	**52**
R	Inferior Parietal Lobule		4.39E-07	52	−56	52
R	Inferior Temporal Gyrus		8.30E-07	58	−48	−14
L	**Middle Temporal Gyrus**	**6845**	**9.79E-07***	**−62**	**−46**	**−14**
L	Inferior Parietal Lobule		1.74E-06	−60	−44	48
L	Middle Temporal Gyrus		6.41E-06	−52	−70	22
L	**Precuneus**	**4067**	**5.15E-06***	**0**	**−68**	**44**
L	Cingulate Gyrus		5.64E-06	−2	−34	30
L	Precuneus		0.0002	−6	−46	34
L	**Caudate**	**125**	**0.0003**	**−10**	**10**	**8**
L	**Middle Frontal Gyrus**	**347**	**0.0009**	**−26**	**28**	**60**
L	Superior Frontal Gyrus		0.0014	−16	10	76
L	Middle Frontal Gyrus		0.0004	−30	14	64
R	**Middle Frontal Gyrus**	**460**	**0.0006**	**38**	**12**	**64**
R	Middle Frontal Gyrus		0.0007	44	4	66

Results are listed at $p < .005$ uncorrected and a cluster size threshold of 100 continuous voxels. Bold data indicate primary peaks within a cluster, non-bold data indicate secondary peaks within the cluster. *MNI*: Montreal Neurological Institute; *p(unc)*: uncorrected p-value; *k*: cluster size.

* $p < .05$ FWE corrected on the cluster-level.

brain morphometry with detailed characterization of the spatial dynamics of brain atrophy in AD. Here, affirmative to studies of brain metabolism, asymmetric patterns of gray matter loss in AD with a left hemispheric pronunciation were demonstrated (Janke et al. 2001; Thompson et al. 1998, 2001). Specific focus has also been given to the hippocampus with meta-analyses showing a consistent left-less-than-right hippocampal volume in MCI and AD patients but also control subjects. While effect sizes were the strongest in MCI subjects, these results indicate dynamic changes of physiological asymmetry patterns during the course of the disease (Shi et al. 2009). On the other hand, Derflinger et al. argued that findings of left lateralized AD pathology are mainly attributable to a selection bias introduced by largely language based cognitive assessments (Derflinger et al. 2011). In our sample post-hoc regression analyses showed that 24-month cognitive decline (ADAS-cog) was significantly associated with rCMRgl decline in both dementia-AD and MCI-AD subjects with patterns closely resembling the results from our group comparisons. Whereas for dementia-AD subjects bilateral decline with at most weak right hemispheric lateralization was seen, evidence of strong left hemispheric lateralization was found for associations of cognitive decline with rCMRgl declines in MCI-AD patients. For both MCI and AD subjects cognitive deficits at baseline and longitudinal decline of the ADAS-cog subitems were most pronounced in tests representative of memory performance, processing speed and praxis while language functions were only modestly affected at baseline and decline was only evident in dementia-AD but not MCI-AD patients, overall consistent with ADNI's focus on memory impairment (Petersen et al. 2010). Similar results were obtained when subitems were grouped to subdomains (i.e. memory, language, praxis), again without significant decline of the language subdomain in MCI-AD subjects. While ADAS-cog provides a general measure of cognitive function we additionally analyzed Category Fluency (animals), a more language focused cognitive assessment of semantic fluency, with known left lateralization in healthy subjects as well as AD patients (Gutierrez-Sigut et al. 2015; Meinzer et al. 2009; Yeung et al. 2016; Zahn et al. 2004). Here, we did find weak but significant 24-month decline in both dementia-AD and MCI-AD with regression analyses yielding strong left hemispheric lateralization for the respective associations with rCMRgl decline, confirmatory to previous reports (Zahn et al. 2004). Nevertheless, in MCI-AD subjects, these associations did not reach statistical significance (all $p > .6$ FWE_c) with the largest cluster located within subcortical structures (i.e. caudate nucleus).

Overall, these findings suggest that left hemispheric rCMRgl declines in our sample of MCI-AD subjects are not the primary result of a selection bias due to earlier detection of language impairment and/or predominant decline of language functions.

Thus far, no clear-cut explanation or potential mechanism has been provided for why left hemispheric brain regions could be more susceptible towards AD related neurodegeneration. Strong evidence indicates that brain regions associated with the default mode network (DMN) – a network of distinct brain regions characterized by increased activity under resting conditions – are particularly affected by AD pathology (Greicius et al. 2003).

This in turn lead to the hypothesis that acquired lifetime cerebral metabolism of DMN regions facilitates AD related pathophysiological mechanisms, thus providing a potential explanation for the selective neuronal vulnerability that is seen in AD (Buckner et al. 2005). Indeed, earliest Aβ accumulation appears to manifest mainly within medial brain regions that form part of the DMN, while later stages of Aβ accumulation include large parts of the neocortex (Palmqvist et al. 2017). Brain regions of the DMN – next to others – include the PCC, precuneus as well as lateral and medial temporal lobe structures. Intriguingly, two studies focusing on the lateralization of DMN activity in healthy subjects showed left hemispheric lateralization, potentially supporting our and previous observations of left lateralized pathology in MCI (Agcaoglu et al. 2015; Swanson et al. 2011). However, AD seems to be characterized by diverging trajectories of regional Aβ pathology and brain metabolic declines (Perani 2014) and although DMN alterations are well established in AD (Pievani et al. 2017), it still remains to be clarified whether these changes develop in an asymmetric or even lateralized manner. Hence further research is required to shed light on the intricate interplay of pathophysiological processes that may lead to a potentially lateralized selective neuronal vulnerability in AD.

Potential support for a higher left hemispheric susceptibility towards AD related neurodegeneration may also be provided by the logopenic variant of primary progressive aphasia (lpPPA), a focal variant of AD with typical AD pathology and distinct patterns of left lateralized temporoparietal atrophy and hypometabolism (Galton et al. 2000; Gorno-Tempini et al. 2004; Henry and Gorno-Tempini 2010; Madhavan et al. 2013; Rohrer et al. 2012). Of note though, other focal variants such as the posterior cortical atrophy exist, that do not present with obvious lateralized pathological hallmarks (Ossenkoppele et al. 2015).

Somewhat contrasting, we found weak respectively strong right hemispheric lateralization in AD patients when compared to healthy controls and MCI-AD patients, indicating that metabolic differences between hemispheres develop in a dynamic fashion and seem to diminish with further progression of the disease. This discrepancy needs to be interpreted under consideration of current theories on mechanisms related to disease progression. Both animal and human research support the concept of AD pathology spreading via neuronal transport and transsynaptic diffusion within interconnected brain regions (such as the DMN) which – in theory- would allow for interhemispheric spreading of to begin with more lateralized pathological changes such as Aβ deposition and TAU formation (Jucker and Walker 2013; Walker et al. 2013).

Several limitations of our study need to be acknowledged. First, this is an exploratory study of preexisting data. However, this limitation is compensated for by the detailed characterization of patients and controls of the ADNI cohort, its comparably large sample sizes and the longitudinal data. We also acknowledge the fact that evidence for strong left hemispheric lateralization was only seen in MCI-AD patients when compared to CU, while within group analyses showed same-directional but weaker effects. Nevertheless, comparisons against control subjects are mandatory as over time rCMRgl declines in healthy subjects as well and hence needs to be controlled for in order to distinguish AD related pathology from effects related to normal aging (Berti et al. 2014). In this context we also want to stress that by the inclusion of

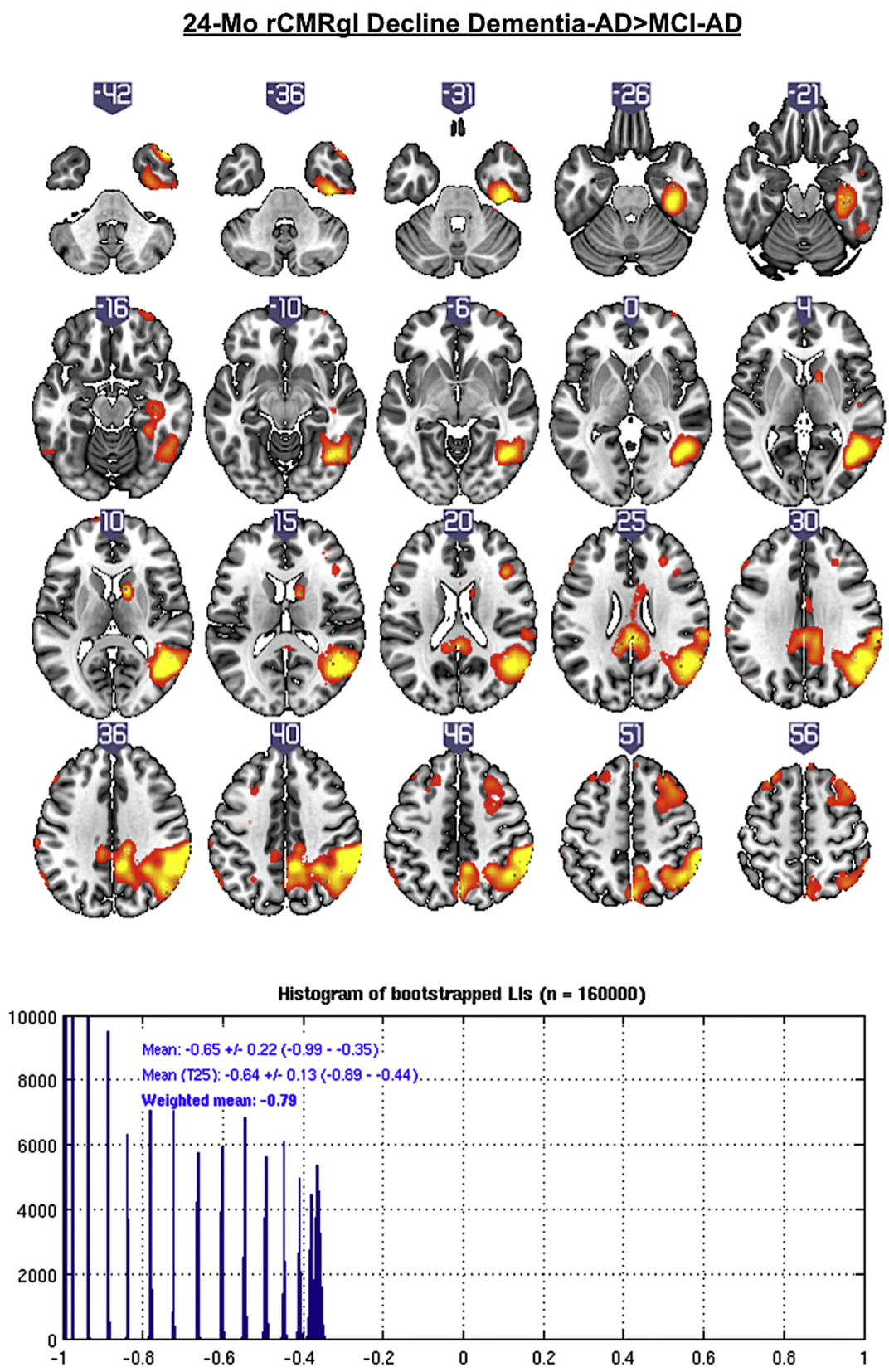

Fig. 4. T-score maps ($p < .005$ uncorrected) of greater 24-month rCMRgl declines in amyloid-β positive dementia-AD patients compared to amyloid-β positive MCI-AD patients with the corresponding histogram of bootstrapped lateralization indices (LIs).

exclusively MCI and AD patients with, and control subjects without evidence of Aβ pathology high specificity of our findings with respect to AD as probable cause is ensured. However, as Aβ pathology was determined based on availability of CSF measures or AV-45 PET imaging data, additional analyses to investigate the relationship between regional amyloid burden and rCMRgl declines in the context of

Table 4
24-month rCMRgl declines in amyloid-β positive dementia-AD patients compared to amyloid-β positive MCI-AD patients.

Region		*k*	p(unc)	MNI (mm)		
				x	y	z
R	**Middle Temporal Gyrus**	**15,732**	**2.70E-06***	**46**	**−60**	**10**
R	Inferior Parietal Lobule		4.17E-06	68	−34	46
R	Inferior Parietal Lobule		5.82E-06	60	−40	46
L	**Superior Frontal Gyrus**	**832**	**0.0001**	**−24**	**6**	**74**
L	Middle Frontal Gyrus		0.0003	−30	24	60
L	Middle Frontal Gyrus		0.0010	−24	32	56
R	**Superior Frontal Gyrus**	**1973**	**0.0002***	**18**	**16**	**74**
R	Middle Frontal Gyrus		0.0005	38	18	54
R	Middle Frontal Gyrus		0.0007	30	26	50
R	**Superior Frontal Gyrus**	**445**	**0.0002**	**26**	**64**	**−22**
R	Middle Frontal Gyrus		0.0008	40	48	−22
R	Middle Frontal Gyrus		0.0017	38	64	−2
L	**Middle Frontal Gyrus**	**181**	**0.0002**	**−56**	**30**	**26**
R	**Subgyral White Matter**	**144**	**0.0004**	**42**	**24**	**20**
L	**Supramarginal Gyrus**	**219**	**0.0005**	**−62**	**−60**	**40**

Results are listed at $p < .005$ uncorrected and a cluster size threshold of 100 continuous voxels. Bold data indicate primary peaks within a cluster, non-bold data indicate secondary peaks within the cluster. *MNI*: Montreal Neurological Institute; *p(unc)*: uncorrected p-value; *k*: cluster size.

* $p < .05$ FWE corrected on the cluster-level.

hemispheric lateralization were not feasible in this sample, a question that should be addressed by future studies.

5. Conclusion

We found left lateralized 24-month rCMRgl declines in Aβ positive persons with MCI, which are not apparent in the dementia stages of AD. It remains to be clarified whether this decline reflects preferential vulnerability to the early stages of AD or neurodegenerative patterns that account for the clinical (e.g. verbal memory) features of MCI.

Acknowledgements

Data collection and sharing for this project was funded by the Alzheimer's Disease Neuroimaging Initiative (ADNI) (National Institutes of Health Grant U01 AG024904) and DOD ADNI (Department of Defense award number W81XWH-12-2-0012). ADNI is funded by the National Institute on Aging, the National Institute of Biomedical Imaging and Bioengineering, and through generous contributions from the following: AbbVie, Alzheimer's Association; Alzheimer's Drug Discovery Foundation; Araclon Biotech; BioClinica, Inc.; Biogen; Bristol-Myers Squibb Company; CereSpir, Inc.; Cogstate; Eisai Inc.; Elan Pharmaceuticals, Inc.; Eli Lilly and Company; EuroImmun; F. Hoffmann-La Roche Ltd and its affiliated company Genentech, Inc.; Fujirebio; GE Healthcare; IXICO Ltd.;Janssen Alzheimer Immunotherapy Research & Development, LLC.; Johnson & Johnson Pharmaceutical Research & Development LLC.; Lumosity; Lundbeck; Merck & Co., Inc.;Meso Scale Diagnostics, LLC.; NeuroRx Research; Neurotrack Technologies; Novartis Pharmaceuticals Corporation; Pfizer Inc.; Piramal Imaging; Servier; Takeda Pharmaceutical Company; and Transition Therapeutics. The Canadian Institutes of Health Research is providing funds to support ADNI clinical sites in Canada. Private sector contributions are facilitated by the Foundation for the National Institutes of Health (www.fnih.org). The grantee organization is the Northern California Institute for Research and Education, and the study is coordinated by the Alzheimer's Therapeutic Research Institute at the University of Southern California. ADNI data are disseminated by the Laboratory for Neuro Imaging at the University of Southern California.

NIH APOE4 grant, “Brain Imaging, APOE and the Preclinical Course of Alzheimer's Disease” (R01AG031581).

ADCC grant,“ Alzheimer's Disease Core Center” (P30AG019610).

API 1, “Alzheimer's Prevention Initiative” (RF1AG041705).

API 2, “Alzheimer's Prevention Initiative APOE4 Trial” (UF1AG046150).

ADNI grant (# 5U01AG024904).

And the State of Arizona (ADHS14-052688).

The authors declare no conflict of interest.

Appendix A. Supplementary data

Supplementary data to this article can be found online at https://doi.org/10.1016/j.nicl.2018.07.016.

References

Agcaoglu, O., Miller, R., Mayer, A.R., Hugdahl, K., Calhoun, V.D., 2015. Lateralization of resting state networks and relationship to age and gender. NeuroImage 104, 310–325. https://doi.org/10.1016/j.neuroimage.2014.09.001.

Berti, V., Mosconi, L., Pupi, A., 2014. Brain: Normal variations and benign findings in FDG PET/CT imaging. PET Clin. 9, 129–140. https://doi.org/10.1016/j.cpet.2013.10.006.

Buckner, R.L., Snyder, A.Z., Shannon, B.J., Larossa, G., Sachs, R., Fotenos, A.F., Sheline, Y.I., Klunk, W.E., Mathis, C.A., Morris, J.C., Mintun, M.A., 2005. Molecular, structural, and functional characterization of Alzheimer's disease: evidence for a relationship between default activity, amyloid, and memory. J. Neurosci. 25, 7709–7717. https://doi.org/10.1523/JNEUROSCI.2177-05.2005.

Claassen, D.O., McDonell, K.E., Donahue, M., Rawal, S., Wylie, S.A., Neimat, J.S., Kang, H., Hedera, P., Zald, D., Landman, B., Dawant, B., Rane, S., 2016. Cortical asymmetry in Parkinson's disease: early susceptibility of the left hemisphere. Brain Behav. 6. https://doi.org/10.1002/brb3.573.

De Winter, F.-L., Zhu, Q., Van den Stock, J., Nelissen, K., Peeters, R., de Gelder, B., Vanduffel, W., Vandenbulcke, M., 2015. Lateralization for dynamic facial expressions in human superior temporal sulcus. NeuroImage 106, 340–352. https://doi.org/10.1016/j.neuroimage.2014.11.020.

Derflinger, S., Sorg, C., Gaser, C., Myers, N., Arsic, M., Kurz, A., Zimmer, C., Wohlschläger, A., Mühlau, M., 2011. Grey-matter atrophy in Alzheimer's disease is asymmetric but not lateralized. J. Alzheimers Dis. 25, 347–357. https://doi.org/10.3233/JAD-2011-110041.

Folstein, M.F., Folstein, S.E., McHugh, P.R., 1975. “Mini-mental state”. A practical method for grading the cognitive state of patients for the clinician. J. Psychiatr. Res. 12, 189–198.

Friedland, R.P., Budinger, T.F., Koss, E., Ober, B.A., 1985. Alzheimer's disease: anterior-posterior and lateral hemispheric alterations in cortical glucose utilization. Neurosci. Lett. 53, 235–240.

Galton, C.J., Patterson, K., Xuereb, J.H., Hodges, J.R., 2000. Atypical and typical presentations of Alzheimer's disease: a clinical, neuropsychological, neuroimaging and pathological study of 13 cases. Brain 123, 484–498. https://doi.org/10.1093/brain/123.3.484.

Gorno-Tempini, M.L., Dronkers, N.F., Rankin, K.P., Ogar, J.M., Phengrasamy, L., Rosen, H.J., Johnson, J.K., Weiner, M.W., Miller, B.L., 2004. Cognition and anatomy in three variants of primary progressive aphasia. Ann. Neurol. 55, 335–346. https://doi.org/10.1002/ana.10825.

Greicius, M.D., Krasnow, B., Reiss, A.L., Menon, V., 2003. Functional connectivity in the resting brain: a network analysis of the default mode hypothesis. Proc. Natl. Acad. Sci. U. S. A. 100, 253–258. https://doi.org/10.1073/pnas.0135058100.

Gutierrez-Sigut, E., Payne, H., MacSweeney, M., 2015. Investigating language lateralization during phonological and semantic fluency tasks using functional transcranial Doppler sonography. Laterality Asymmetries Body Brain Cogn. 20, 49–68. https://doi.org/10.1080/1357650X.2014.914950.

Haxby, J.V., Duara, R., Grady, C.L., Cutler, N.R., Rapoport, S.I., 1985. Relations between neuropsychological and cerebral metabolic asymmetries in early Alzheimer's disease. J. Cereb. Blood Flow Metab. 5, 193–200. https://doi.org/10.1038/jcbfm.1985.25.

Henry, M.L., Gorno-Tempini, M.L., 2010. The logopenic variant of primary progressive aphasia. Curr. Opin. Neurol. 23, 633–637. https://doi.org/10.1097/WCO.0b013e32833fb93e.

Herholz, K., Ebmeier, K., 2011. Clinical amyloid imaging in Alzheimer's disease. Lancet Neurol. 10, 667–670. https://doi.org/10.1016/S1474-4422(11)70123-5.

Ibáñez, V., Pietrini, P., Alexander, G.E., Furey, M.L., Teichberg, D., Rajapakse, J.C., Rapoport, S.I., Schapiro, M.B., Horwitz, B., 1998. Regional glucose metabolic abnormalities are not the result of atrophy in Alzheimer's disease. Neurology 50, 1585–1593. https://doi.org/10.1212/WNL.50.6.1585.

Jack, C.R., Knopman, D.S., Jagust, W.J., Shaw, L.M., Aisen, P.S., Weiner, M.W., Petersen, R.C., Trojanowski, J.Q., 2010. Hypothetical model of dynamic biomarkers of the Alzheimer's pathological cascade. Lancet Neurol. 9, 119–128. https://doi.org/10.1016/S1474-4422(09)70299-6.

Jack, C.R., Albert, M.S., Knopman, D.S., McKhann, G.M., Sperling, R.A., Carrillo, M.C., Thies, B., Phelps, C.H., 2011. Introduction to the recommendations from the National Institute on Aging-Alzheimer's Association workgroups on diagnostic guidelines for Alzheimer's disease. Alzheimers Dement. J. Alzheimers Assoc. 7, 257–262. https://doi.org/10.1016/j.jalz.2011.03.004.

Jack, C.R., Bennett, D.A., Blennow, K., Carrillo, M.C., Dunn, B., Haeberlein, S.B.,

Holtzman, D.M., Jagust, W., Jessen, F., Karlawish, J., Liu, E., Molinuevo, J.L., Montine, T., Phelps, C., Rankin, K.P., Rowe, C.C., Scheltens, P., Siemers, E., Snyder, H.M., Sperling, R., Elliott, C., Masliah, E., Ryan, L., Silverberg, N., 2018. NIA-AA research framework: toward a biological definition of Alzheimer's disease. Alzheimers Dement. J. Alzheimers Assoc. 14, 535–562. https://doi.org/10.1016/j.jalz.2018.02.018.

Janke, A.L., de Zubicaray, G., Rose, S.E., Griffin, M., Chalk, J.B., Galloway, G.J., 2001. 4D deformation modeling of cortical disease progression in Alzheimer's dementia. Magn. Reson. Med. 46, 661–666.

Janota, I., Mountjoy, C.Q., 1988. Asymmetry of pathology in Alzheimer's disease. J. Neurol. Neurosurg. Psychiatry 51, 1011–1012.

Jucker, M., Walker, L.C., 2013. Self-propagation of pathogenic protein aggregates in neurodegenerative diseases. Nature 501, 45–51. https://doi.org/10.1038/nature12481.

Keilp, J.G., Alexander, G.E., Stern, Y., Prohovnik, I., 1996. Inferior parietal perfusion, lateralization, and neuropsychological dysfunction in Alzheimer's disease. Brain Cogn. 32, 365–383. https://doi.org/10.1006/brcg.1996.0071.

Loewenstein, D.A., Barker, W.W., Chang, J.Y., Apicella, A., Yoshii, F., Kothari, P., Levin, B., Duara, R., 1989. Predominant left hemisphere metabolic dysfunction in dementia. Arch. Neurol. 46, 146–152.

Madhavan, A., Whitwell, J.L., Weigand, S.D., Duffy, J.R., Strand, E.A., Machulda, M.M., Tosakulwong, N., Senjem, M.L., Gunter, J.L., Lowe, V.J., Petersen, R.C., Jack, C.R., Josephs, K.A., 2013. FDG PET and MRI in Logopenic primary progressive aphasia versus dementia of the Alzheimer's type. PLoS One 8. https://doi.org/10.1371/journal.pone.0062471.

Meinzer, M., Wilser, L., Flaisch, T., Eulitz, C., Rockstroh, B., Conway, T., Rothi, L.J.G., Crosson, B., 2009. Neural signatures of semantic and phonemic fluency in young and old adults. J. Cogn. Neurosci. 21, 2007–2018. https://doi.org/10.1162/jocn.2009.21219.

Mohs, R.C., Knopman, D., Petersen, R.C., Ferris, S.H., Ernesto, C., Grundman, M., Sano, M., Bieliauskas, L., Geldmacher, D., Clark, C., Thal, L.J., 1997. Development of cognitive instruments for use in clinical trials of antidementia drugs: additions to the Alzheimer's disease assessment scale that broaden its scope. The Alzheimer's Disease Cooperative Study. Alzheimer Dis. Assoc. Disord. 11 (Suppl 2), S13–S21.

Morris, J.C., 1993. The clinical dementia rating (CDR): current version and scoring rules. Neurology 43, 2412–2414.

Mosconi, L., 2013. Glucose metabolism in normal aging and Alzheimer's disease: methodological and physiological considerations for PET studies. Clin. Transl. Imaging Rev. Nucl. Med. Mol. Imaging 1. https://doi.org/10.1007/s40336-013-0026-y.

Ossenkoppele, R., Cohn-Sheehy, B.I., La Joie, R., Vogel, J.W., Möller, C., Lehmann, M., van Berckel, B.N.M., Seeley, W.W., Pijnenburg, Y.A., Gorno-Tempini, M.L., Kramer, J.H., Barkhof, F., Rosen, H.J., van der Flier, W.M., Jagust, W.J., Miller, B.L., Scheltens, P., Rabinovici, G.D., 2015. Atrophy patterns in early clinical stages across distinct phenotypes of Alzheimer's disease. Hum. Brain Mapp. 36, 4421–4437. https://doi.org/10.1002/hbm.22927.

Palmqvist, S., Schöll, M., Strandberg, O., Mattsson, N., Stomrud, E., Zetterberg, H., Blennow, K., Landau, S., Jagust, W., Hansson, O., 2017. Earliest accumulation of β-amyloid occurs within the default-mode network and concurrently affects brain connectivity. Nat. Commun. 8 (1214). https://doi.org/10.1038/s41467-017-01150-x.

Perani, D., 2014. FDG-PET and amyloid-PET imaging: the diverging paths. Curr. Opin. Neurol. 27, 405–413. https://doi.org/10.1097/WCO.0000000000000109.

Petersen, R.C., Aisen, P.S., Beckett, L.A., Donohue, M.C., Gamst, A.C., Harvey, D.J., Jack, C.R., Jagust, W.J., Shaw, L.M., Toga, A.W., Trojanowski, J.Q., Weiner, M.W., 2010. Alzheimer's disease neuroimaging initiative (ADNI): clinical characterization. Neurology 74, 201–209. https://doi.org/10.1212/WNL.0b013e3181cb3e25.

Pievani, M., Pini, L., Ferrari, C., Pizzini, F.B., Boscolo Galazzo, I., Cobelli, C., Cotelli, M., Manenti, R., Frisoni, G.B., 2017. Coordinate-based meta-analysis of the default mode and salience network for target identification in non-invasive brain stimulation of Alzheimer's disease and behavioral variant frontotemporal dementia networks. J. Alzheimers Dis. 57, 825–843. https://doi.org/10.3233/JAD-161105.

Raji, C.A., Becker, J.T., Tsopelas, N.D., Price, J.C., Mathis, C.A., Saxton, J.A., Lopresti, B.J., Hoge, J.A., Ziolko, S.K., Dekosky, S.T., Klunk, W.E., 2008. Characterizing regional correlation, laterality and symmetry of amyloid deposition in mild cognitive impairment and Alzheimer's disease with Pittsburgh compound B. J. Neurosci. Methods 172, 277–282. https://doi.org/10.1016/j.jneumeth.2008.05.005.

Reiman, E.M., Jagust, W.J., 2012. Brain imaging in the study of Alzheimer's disease. NeuroImage 61, 505–516. https://doi.org/10.1016/j.neuroimage.2011.11.075.

Rey, A., 1964. L'examen Clinique en Psychologie. Presses Universitaires de France, Paris.

Rohrer, J.D., Rossor, M.N., Warren, J.D., 2012. Alzheimer's pathology in primary progressive aphasia. Neurobiol. Aging 33, 744–752. https://doi.org/10.1016/j.neurobiolaging.2010.05.020.

Rosen, W.G., 1980. Verbal fluency in aging and dementia. J. Clin. Neuropsychol. 2, 135–146. https://doi.org/10.1080/01688638008403788.

Rosen, W.G., Mohs, R.C., Davis, K.L., 1984. A new rating scale for Alzheimer's disease. Am. J. Psychiatry 141, 1356–1364. https://doi.org/10.1176/ajp.141.11.1356.

Saint-Aubert, L., Lemoine, L., Chiotis, K., Leuzy, A., Rodriguez-Vieitez, E., Nordberg, A., 2017. Tau PET imaging: present and future directions. Mol. Neurodegener. 12. https://doi.org/10.1186/s13024-017-0162-3.

Shi, F., Liu, B., Zhou, Y., Yu, C., Jiang, T., 2009. Hippocampal volume and asymmetry in mild cognitive impairment and Alzheimer's disease: meta-analyses of MRI studies. Hippocampus 19, 1055–1064. https://doi.org/10.1002/hipo.20573.

Siegel, B.V., Shihabuddin, L., Buchsbaum, M.S., Starr, A., Haier, R.J., Valladares Neto, D.C., 1996. Gender differences in cortical glucose metabolism in Alzheimer's disease and normal aging. J. Neuropsychiatry Clin. Neurosci. 8, 211–214. https://doi.org/10.1176/jnp.8.2.211.

Small, G.W., Mazziotta, J.C., Collins, M.T., Baxter, L.R., Phelps, M.E., Mandelkern, M.A., Kaplan, A., La Rue, A., Adamson, C.F., Chang, L., 1995. Apolipoprotein E type 4 allele and cerebral glucose metabolism in relatives at risk for familial Alzheimer disease. JAMA 273, 942–947.

Swanson, N., Eichele, T., Pearlson, G., Kiehl, K., Yu, Q., Calhoun, V.D., 2011. Lateral differences in the default mode network in healthy controls and schizophrenia patients. Hum. Brain Mapp. 32, 654–664. https://doi.org/10.1002/hbm.21055.

Thompson, P.M., Moussai, J., Zohoori, S., Goldkorn, A., Khan, A.A., Mega, M.S., Small, G.W., Cummings, J.L., Toga, A.W., 1998. Cortical variability and asymmetry in normal aging and Alzheimer's disease. Cereb. Cortex 8, 492–509. https://doi.org/10.1093/cercor/8.6.492.

Thompson, P.M., Mega, M.S., Woods, R.P., Zoumalan, C.I., Lindshield, C.J., Blanton, R.E., Moussai, J., Holmes, C.J., Cummings, J.L., Toga, A.W., 2001. Cortical change in Alzheimer's disease detected with a disease-specific population-based brain atlas. Cereb. Cortex N. Y. N 1991 (11), 1–16.

Volkow, N.D., Zhu, W., Felder, C.A., Mueller, K., Welsh, T.F., Wang, G.J., de Leon, M.J., 2002. Changes in brain functional homogeneity in subjects with Alzheimer's disease. Psychiatry Res. 114, 39–50.

Walker, L.C., Diamond, M.I., Duff, K.E., Hyman, B.T., 2013. Mechanisms of protein seeding in neurodegenerative diseases. JAMA Neurol. 70, 304–310. https://doi.org/10.1001/jamaneurol.2013.1453.

Wilcock, G.K., Esiri, M.M., 1987. Asymmetry of pathology in Alzheimer's disease. J. Neurol. Neurosurg. Psychiatry 50, 1384–1386.

Wilke, M., Lidzba, K., 2007. LI-tool: a new toolbox to assess lateralization in functional MR-data. J. Neurosci. Methods 163, 128–136. https://doi.org/10.1016/j.jneumeth.2007.01.026.

Yeung, M.K., Sze, S.L., Woo, J., Kwok, T., Shum, D.H.K., Yu, R., Chan, A.S., 2016. Altered frontal lateralization underlies the category fluency deficits in older adults with mild cognitive impairment: a near-infrared spectroscopy study. Front. Aging Neurosci. 8. https://doi.org/10.3389/fnagi.2016.00059.

Zahn, R., Juengling, F., Bubrowski, P., Jost, E., Dykierek, P., Talazko, J., Huell, M., 2004. Hemispheric asymmetries of hypometabolism associated with semantic memory impairment in Alzheimer's disease: a study using positron emission tomography with fluorodeoxyglucose-F18. Psychiatry Res. Neuroimaging 132, 159–172. https://doi.org/10.1016/j.pscychresns.2004.07.006.